

Detection of butt weld of laser-MIG hybrid welding of thin-walled profile for high-speed train

Qingxiang Zhou

*Technical Engineering Department, CRRC Qingdao Si Fang Co., Ltd,
Qingdao, China, and*

Fang Liu, Jingming Li, Jiankui Li, Shuangnan Zhang and Guixi Cai
*Analysis and Testing Center, Institute of Metal Research,
Chinese Academy of Sciences, Shenyang, China*

Abstract

Purpose – This study aims to solve the problem of weld quality inspection, for the aluminum alloy profile welding structure of high-speed train body has complex internal shape and thin plate thickness (2–4 mm), the conventional nondestructive testing method of weld quality is difficult to implement.

Design/methodology/approach – In order to solve this problem, the ultrasonic creeping wave detection technology was proposed. The impact of the profile structure on the creeping wave detection was studied by designing profile structural test blocks and artificial simulation defect test blocks. The detection technology was used to test the actual welded test blocks, and compared with the results of X-ray test and destructive test (tensile test) to verify the accuracy of the ultrasonic creeping wave test results.

Findings – It is indicated that that X-ray has better effect on the inspection of porosities and incomplete penetration defects. However, due to special detection method and protection, the detection speed is slow, which cannot meet the requirements of field inspection of the welding structure of aluminum alloy thin-walled profile for high-speed train body. It can be used as an auxiliary detection method for a small number of sampling inspection. The ultrasonic creeping wave can be used to detect the incomplete penetration welds with the equivalent of 0.25 mm or more, the results of creeping wave detection correspond well with the actual incomplete penetration defects.

Originality/value – The results show that creeping wave detection results correspond well with the actual non-penetration defects and can be used for welding quality inspection of aluminum alloy thin-wall profile composite welding joints. It is recommended to use the echo amplitude of the 10 mm × 0.2 mm × 0.5 mm notch as the criterion for weld qualification.

Keywords High-speed train, Aluminum alloy profile, Laser-MIG hybrid welding, Nondestructive inspection, X-ray radiography, Ultrasonic creeping wave detection

Paper type Technical paper

1. Introduction

Li and Han (2004) proposed that with the rapid development of China's high-speed railway, body lightweight has become a key technology to improve the speed of train operation through the research of stainless steel body welding technology and its development. Through the study of laser-MIG composite welding process, Chen, Gou, Zhu, Yang and Xiong (2015) found that aluminum and its alloy products have been widely used due to their lightweight, high-specific strength, corrosion resistance, high plasticity, performance close to



or even exceed some high-quality steels, and easy to realize large-scale and wide-body profiles. In recent years, aluminum alloy thin-walled profiles, as key components, have been widely used in high-speed train manufacturing and have partially replaced traditional steel materials. Wang and Chen (2010) and Zhang, Zhan and Ma (2019) proposed that the aluminum alloy welding method of train body has become the basic problem in the field of rail transit manufacturing.

Laser-MIG hybrid welding is to combine laser and MIG arc. On the basis of the advantages of high-energy density, small heat-affected zone and fast welding speed of laser welding, the welding adaptability is improved through the better directivity of MIG, which makes the welding process more stable, the weld bridging property better, the thermal efficiency higher, and larger welding assembly gap is allowed. Meanwhile, as MIG welding itself has relatively stable wire filling performance, it can improve the microstructure of weld metal, and then improve the mechanical performance of weld. However, laser welding and MIG welding are two kinds of welding heat sources with completely different properties, which increases the complexity of parameter selection. Zeng, Shi and Shi (2009) show that unreasonable parameters will lead to some defects. Zhang (2016) through the study of the microstructure and properties of 5754-H32 aluminum alloy laser welding joint, it is found that the selection of unreasonable parameters will lead to the formation of some defects, common defects include the following types: poor weld formation, thermal crack defect, porosity, slag inclusion, incomplete fusion, incomplete penetration defect, etc., among which cracks, incomplete penetration, incomplete fusion and other area defects will lead to stress concentration and great harm, and these defects will directly affect the strength of welds and the safety of high-speed train operation. In order to ensure the welding quality, it is urgent to perform the nondestructive testing and quality evaluation study of the weld performance of laser-MIG hybrid welding.

According to the structural characteristics of butt weld of thin-walled profile for high-speed train, the existing testing standards and ultrasonic testing methods are analyzed, ultrasonic creeping wave detection technology for weld quality inspection of laser-MIG hybrid welding of thin-walled profiles is put forward, i.e. designing and contrasting test blocks to eliminate the influence of welding structure on creeping wave detection. The creeping wave detection technology is used to detect the weld of actual welded test plate, and X-ray testing method, tensile test and weld fracture observation are used for comparison and verification.

2. Detection method for butt weld of thin-wall

The welding structure of aluminum alloy carbody is complex, which is of plug-in type with tie plate profile. The butt weld structure formed by laser-MIG hybrid welding on single side is shown in Figure 1. In the figure, d_1 and d_2 are the thicknesses of two thin-walled profiles; b is the weld width. It can be seen from Figure 1 that the thickness of thin-walled profiles is thin (2–4 mm), the weld width is about 10 mm, and the weld area is very close to the support plate of profile structure. Due to the limitation of plate thickness and detection space, the conventional nondestructive testing method of weld quality is difficult to implement.

2.1 Existing detection methods

At present, the current standards *Arc-welded Joints in Aluminium and its Alloys—Guidance on Quality Levels for Imperfection* (GB/T 22087—2008) and *Electron and Laser Beam Welded Joints—Guidance on Quality Levels for Imperfections—Part 2: Aluminium and its Weldable Alloys* (GB/T 22085.2—2008) provide guiding welding quality reference standards for laser-MIG hybrid welding joints. In terms of welding quality inspection technology and evaluation standards, *Non-destructive Testing of Welds—Acceptance Levels for Radiographic Testing—Part 2: Aluminium and its Alloys* (ISO10675-2—2017) and *Nondestructive Testing of Pressure*

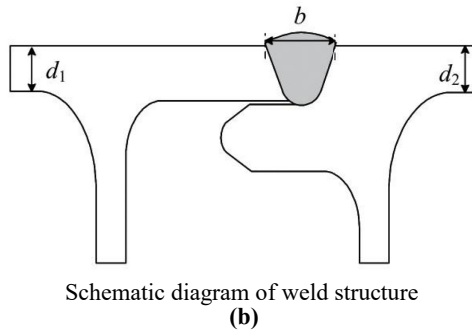
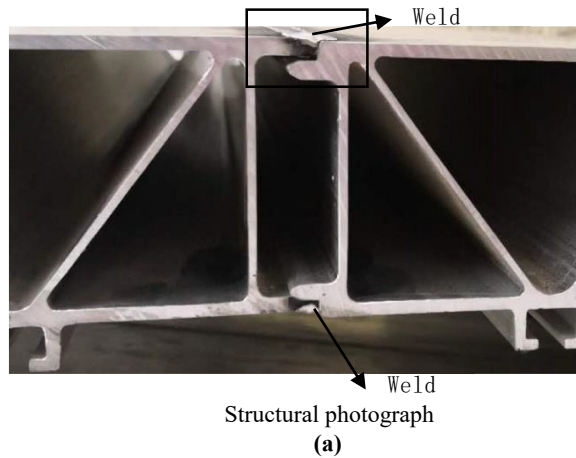


Figure 1.
Laser-MIG hybrid
welding of thin-walled
profile

Equipments Part 2: Radiographic Testing (NB/T 47013.2—2015) stipulates the evaluation of radiographic testing results and quality classification standards for aluminum alloy fusion welding joints. However, considering the safety protection and efficiency, the radiographic inspection method cannot be fully applied to the quality inspection of laser-MIG hybrid welding joint in the rail car production workshop. Therefore, it is very necessary to use advanced nondestructive testing technology to detect and evaluate laser weld of aluminum alloy sheet efficiently, reliably and accurately.

Ultrasonic testing method has the advantages of simple equipment, fast detection speed and high sensitivity, and has high-detection sensitivity for area defects, which has been widely used in butt weld detection of plates, and many detection standards have been established; among them, *Nondestructive Testing of Pressure Equipments—Part 3: Ultrasonic Testing* (NB/T 47013.3—2015) and *Non-destructive Testing of Welds—Ultrasonic Testing—Techniques, Testing Levels, and Assessment* (GB/T 11345—2013) respectively stipulate ultrasonic shear wave testing methods for butt welds with base metal thickness not less than 6 mm and not less than 8 mm. However, the shear wave testing method specified in the standard cannot be applied to the butt weld detection of thin-walled profiles, because the thickness of thin-walled profiles is thin, the sonic path distance of direct wave and primary reflected wave of shear wave is short, which is basically in the near field area of probe sound field, and signal aliasing or in the blind area of detection, so it is extremely

difficult to analyze the results; It is easy to generate “mountain-shaped” pseudo-defect interference wave owing to the influence of excess weld metal when testing butt weld by shear wave, which affects the judgment of defects, especially when testing sheet; When multiple reflected wave is detected by shear wave, the sensitivity of detection will be reduced due to the increase of reflection times and the large energy attenuation.

Other common ultrasonic testing methods, such as phased array testing methods, are generally used for welding quality detection of friction stir welding. Due to the great influence of excess weld metal, the excess weld metal must be leveled during testing; it is difficult to analyze the detection results with ultrasonic Lamb wave detection method as Lamb is sensitive to the change of weld morphology, and modal conversion, dispersion and energy attenuation will occur during propagation; ultrasonic surface wave testing method is sensitive to surface defects, and the excess weld metal and uneven weld bead will interfere with the analysis of testing results. To sum up, the ultrasonic testing methods for butt welds of thin-walled profiles with thickness less than 6 mm need to be improved and new testing technologies will be developed.

2.2 Ultrasonic creeping wave detection technology

Gan, Fang, Yu, Yu and Su (2014), Sony, Balasubramanian and Pardikar (2003) and Zhang and Lian (2010) applied ultrasonic creep wave detection technology to the experimental research and application of butt welding detection of thin-walled pipe. *The Enterprise Standard of State Grid* (2016) and *Power Industry Standard* (2012) stipulate creeping wave detection of thin-walled tubes with thickness ranging from 4 to 8 mm. However, there is little research on the application of butt weld detection for 2-4 mm thick aluminum sheet, and the thin-walled profiles studied in this paper have complicated structure and uneven weld bead surface, which has certain influence on the creeping wave detection effect.

In view of the above analysis, the ultrasonic creeping wave detection technology for butt welds of thin-walled profiles is put forward: design relevant comparison test blocks, calibrate the signal position and amplitude of the weld bead interference and profile structure interference on the testing equipment in advance. Eliminate non-defective signal interference in the test results by setting parameters such as gate position and detection gain during detection. The ultrasonic creeping wave testing technology is adopted to detect the laser-MIG hybrid welding joint of aluminum alloy sheet, and the X-ray testing method and tensile tests are adopted for comparison and verification, which provide references for nondestructive testing of welded joints of aluminum alloy sheet.

The schematic diagram of excitation and propagation of creeping wave in thin-walled profiles is shown in Figure 2. It can be seen from Figure 2 that when the ultrasonic creeping wave probe for aluminum alloy is used and its incidence angle α_i is about 26° , grazing incidence longitudinal wave (L wave) with refracted angle of about 90° will be generated in aluminum alloy sheet. Creeping wave probe generates refracted longitudinal wave L in aluminum alloy sheet at critical incidence angle and propagates in the sheet. When the longitudinal wave propagates to position 1, the wave line of longitudinal wave L is arched-shaped, and wave mode conversion is generated on the upper and lower surfaces of the sheet to form shear wave (S wave) with refracted angle of about 30° ; as the longitudinal wave

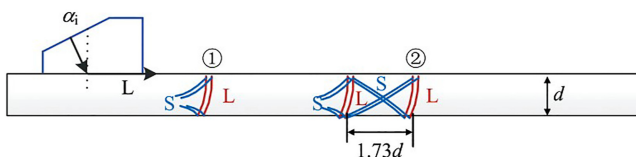


Figure 2.
Schematic diagram of
excitation and
propagation of
creeping wave in thin-
walled profiles

propagates forward, the longitudinal wave L continuously derives the shear wave S, and the S wave also propagates in the sheet; when the longitudinal wave L propagates to the position 2, the derived shear wave S propagates to the opposite side of sheet, and the longitudinal wave L is formed by wave mode conversion again, and finally the X wave structure as shown in the figure is formed. The distance between the two longitudinal wave front is about $1.73d$ (d is the sheet thickness). Cai *et al.* (2018), based on the ultrasonic propagation process, proposes a simplified analysis model of wave line-wave surface dynamic evolution in order to explain the shear wave S derived from the longitudinal wave during propagation is also called the head wave, and the head wave takes the intersection of the longitudinal wave front and the sidewall as the wave source. The wave mode in which the longitudinal wave formed by the grazing incidence longitudinal wave and the head wave propagate at the same time is called the creeping wave.

According to the formation mechanism and propagation characteristics of creeping waves, it can be seen that the longitudinal waves in creeping waves propagate in a direction almost parallel to the sheet surface, which is conducive to finding the cracks between the upper and lower sheet surfaces perpendicular to the surface; the head wave in the creeping wave is equivalent to two shear wave probes with a direction difference of 180° on the upper and lower surfaces of the sheet, which are automatically scanned along the surface of the sheet. Therefore, it can also detect surface defects that are inclined to the surface, especially suitable for detecting sidewalls with incomplete fusion and a groove angle of 30° .

3. Test methods

3.1 Welding test block

Select the welding test blocks of 3 thickness combinations (type A, B and C) in the joint form shown in Figure 1, which are welded by laser-MIG hybrid welding, all of which are single-sided butt welds with tie plate. The material of aluminum alloy sheet is 6106-T6. See Table 1 for specification parameters of butt welds.

The weld on the laser-MIG hybrid welding test block is 8–10 mm wide, and the excess weld metal is about 0.5–0.8 mm.

3.2 X-ray testing

Due to the complex structure of the laser-MIG hybrid welding test block, conventional X-ray testing methods cannot detect the welds on the upper and lower surfaces separately. In order not to damage the test plate, the double-wall double-projection X-ray testing method is adopted. The workpiece to be detected is parallel to the ground, and the X-ray machine is placed on a movable platform at a certain angle (about 55°). The X-ray is taken on the upper surface of the workpiece, and the negative is attached to the lower surface of the workpiece. In this way, two welds are imaged on one negative by radiography, and the images of the two welds do not overlap, thus ensuring the imaging quality. The schematic diagram of double-wall and double-projection X-ray testing method is shown in Figure 3. Due to its low detection efficiency, this method is suitable for review and verification or spot check, and cannot be used as a conventional detection method.

Table 1.
Specification
parameters of
butt welds

Specification	d_1 /mm	d_2 /mm
Type A	2.8	3.4
Type B	2.4	2.6
Type C	2.8	2.4

Multiple welding test blocks shall be tested, and the cumulative length of welds subject to X-ray testing is about 20 m. The test results of the test plate with typical characteristic defects are shown in Figure 4. According to Article 6.2 of NB/T 47013.2—2015, the evaluation results are as follows: continuous incomplete penetration is found in the weld of type A test block; intermittent partial incomplete penetration is found in the weld of type B and type C test blocks. All welds subject to X-ray testing shall be verified through ultrasonic creeping wave detection.

According to the analysis of X-ray testing results of welds with a length of nearly 20 m, incomplete penetration is found to be the major defect in the butt welds of three specifications, accounting for 92% of the total defects while porosity defect for a few. The area shown in the box in Figure 4 is the sampling position for destructive test sample in the next step. Take

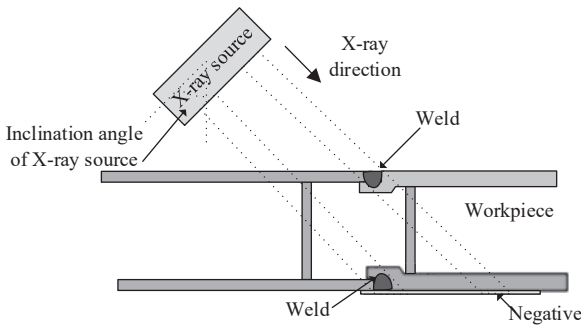
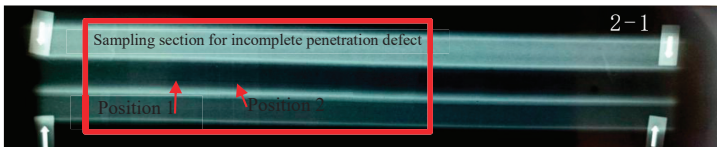
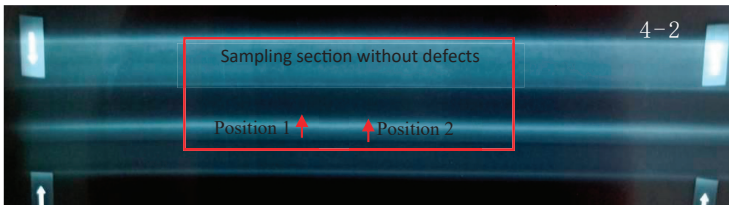


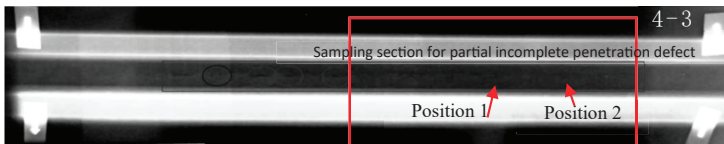
Figure 3.
Schematic diagram of
double-wall and
double-projection
X-ray testing method



Type A
(a)



Type B
(b)



Type C
(c)

Figure 4.
X-ray test results of
butt welds of welding
test blocks of different
specifications

samples in the incomplete penetration area of type A weld, in the area without incomplete penetration defects of type B weld and in the partial incomplete penetration area of type C weld.

3.3 Ultrasonic creeping wave detection

3.3.1 Test block for artificial defects. The reinforcing bar supporting structure on the actual welded structural plate is complex, and the distance from the butt weld is close, and the special design of the structure with tie plate brings adverse effects to ultrasonic detection. In order to study the influence of the complex structure of thin-walled profiles on creeping wave detection, a simulated welding structure test block is designed. The aluminum alloy with the same type as the actual weld is used as raw material, and the same joint structure is machined by wire cutting according to the geometric size of the actual welded joint, as shown in Figure 5, in which the position of the ideal toe of “weld” during actual welding is marked with red-dotted line.

In order to test the detection ability of creeping wave detection method for various defects, artificial simulation defect test block is designed. The raw materials of the test block are taken from the actual profile welding test block with corresponding specifications, and the reinforcement of weld is reserved. By means of electrical discharge machining, crack defects with a depth of 0.25 mm and 0.50 mm are machined on the upper surface of the simulated weld and root incomplete welding defects with a depth of 4.7 mm and 5.2 mm from the lower surface are machined on the lower surface of the simulated weld. Porosity defects inside the weld are simulated by drilling holes on the upper surface of the weld, and the dimension of the test block is shown in Figure 6.

3.3.2 Detection technology. As the actual welding profile sample is shown in Figure 1, it cannot be tested from the opposite side of welding, so only one side can be tested; furthermore, through theoretical analysis and practical detection and verification, it is difficult to separate the structural interference signal from the actual defect signal due to the influence of the tie plate when detection is performed at the tie plate, and the detection effect is not ideal. Therefore, through simulation and optimization test, a special creeping wave probe with a wafer vibration frequency of 5 MHz and a dimension of 6 mm × 4 mm is specially designed and manufactured, and a small wafer with a higher frequency is used to overcome the adverse effect on defect detection caused by the close (only about 8 mm) distance between weld and reinforcing bar. Ultrasonic waves are emitted from a slab side without tie plates to the welded joint area, the front edge of the probe is aligned with the edge of the weld and a straight line scanning is carried out parallel to the edge of the weld. EUT-101C ultrasonic detector is used for detection and testing. First, a group of reflection waveforms caused by structural characteristics of profiles is collected as structural characteristic signals, and the structural

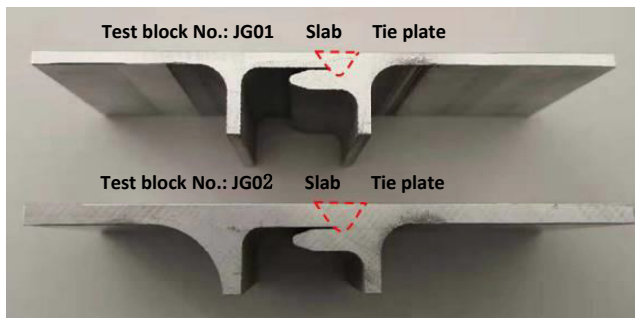


Figure 5.
Simulation of welding
structural test block
with tie plate

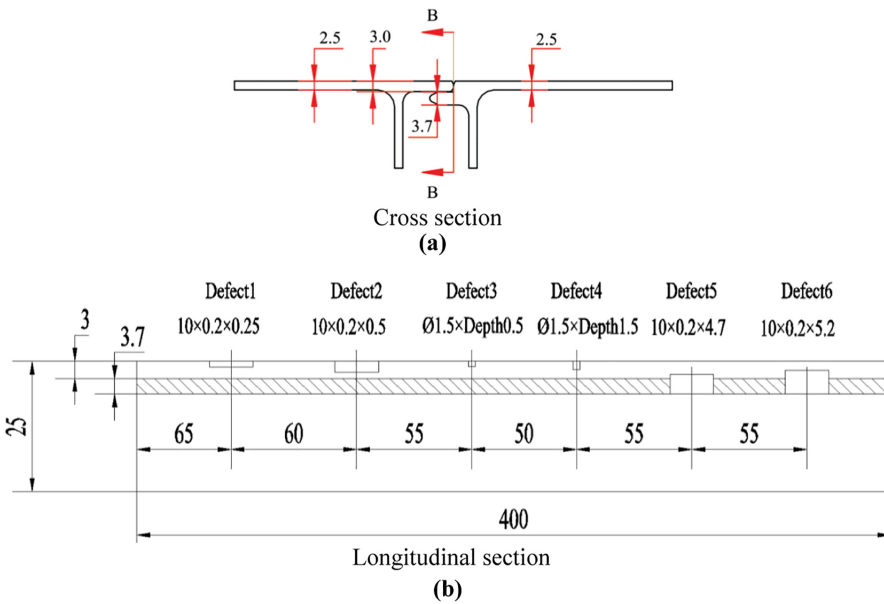
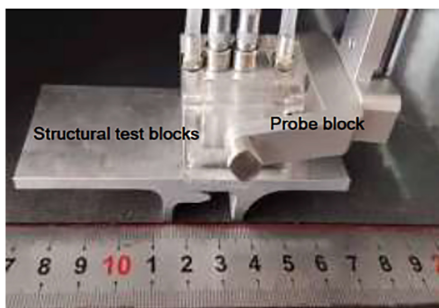


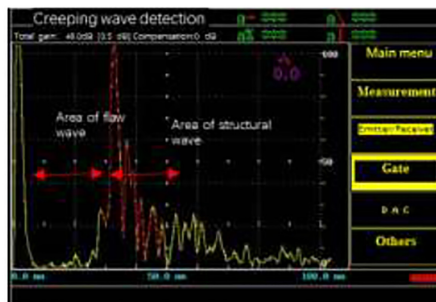
Figure 6. Schematic diagram of contrasting test block welds for artificial defects (unit: mm)

characteristic signals are marked in red on the screen of the instrument by using the “peak holding” function, as shown in Figure 7; then the probe shall be placed on the test block to be tested for the same test. The probe position, instrument parameters and gate settings are consistent with the parameters of the test block (JG-01, JG-02) for weld structure analysis during the test. According to the different positions between the flaw echo and the profile structure echo in time domain, the position and length of the gate can be set accordingly to identify the defects during creeping wave detection.

3.3.3 *Detection result.* With reference to the detection technology of structural test block, six artificial defects on the artificial simulation defect test block are detected, and the detection results are shown in Figure 8. During detection, the area where structural waves appear has been displayed in the A-scan result diagram by using the peak holding function, and the position is about 30 mm on the horizontal scale, so the gate is set accordingly; the



Schematic diagram of structural test block test (a)



Structural characteristic signal calibration (b)

Figure 7. Test result of structural test block

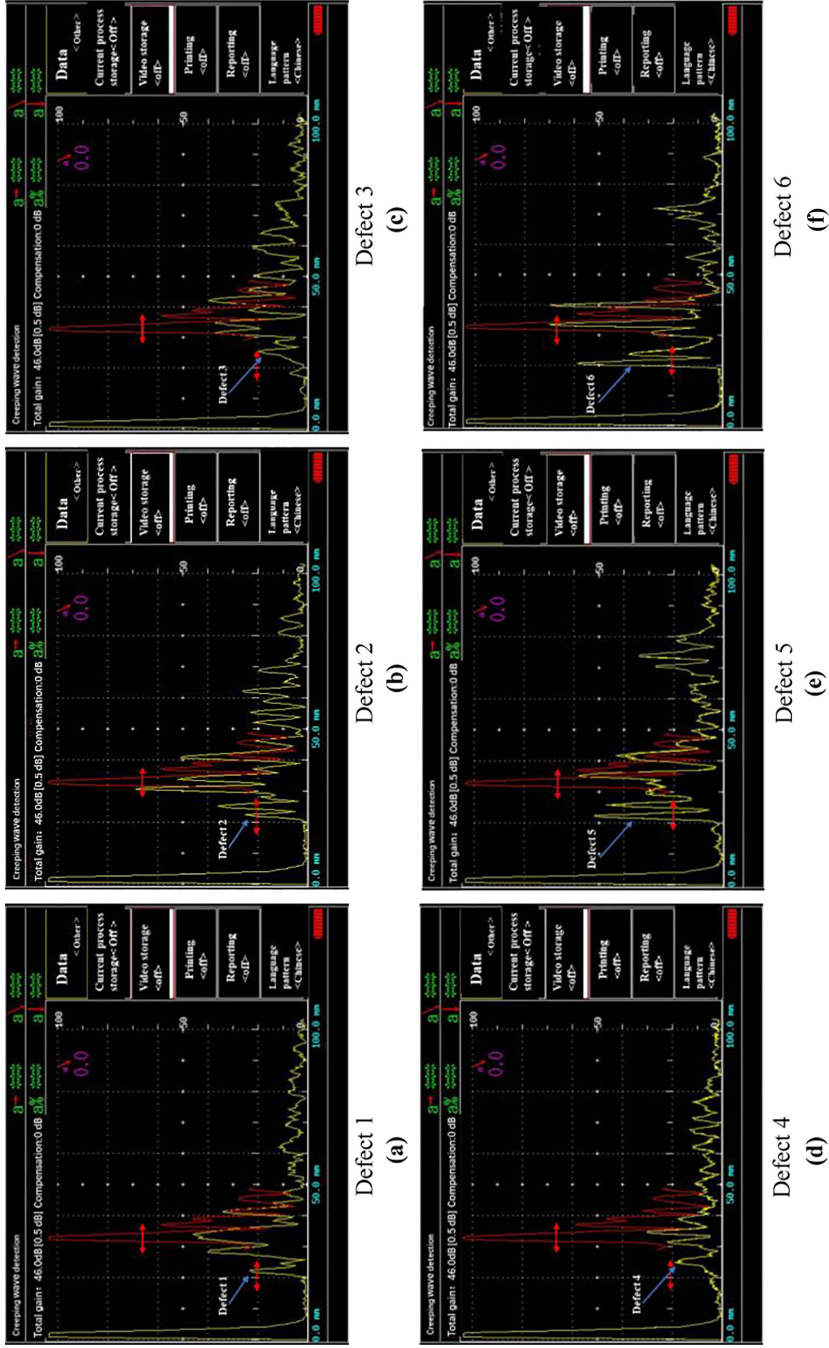


Figure 8. Test results of 6 simulated defects on artificial defect test block

signal appearing in the gate between the initial wave and the structural wave signal is a simulated defect signal. It can be seen from the test results of 0.25 mm grooving in Figure 8(a) and 0.5 mm grooving in Figure 8(b): The amplitude of simulated flaw echo signal increases with the increase of grooving depth. It can be seen from the test results of 0.5 mm deep hole defects in Figure 8(c) and 1.5 mm deep hole defects in Figure 8(d) that with the increase of drilling defect depth, the amplitude of simulated echo wave changes less obviously, but the resolution of echo signal is higher; the test results of 4.7 mm deep incomplete penetration defect in Figure 8(e) and 5.2 mm deep incomplete penetration defect in Figure 8(f) show that with the increase of the size of incomplete penetration depth, the amplitude of simulated flaw echo signal increases; the test results of artificial simulation defect show that creeping wave detection technology has a good detection effect on three kinds of simulated defects.

The creeping wave detection results of destructive samples selected from the weld test blocks of 3 specifications are shown in Figure 9. In the figure, positions 1 and 2 represent the positions of two different typical signals, and the specific positions are shown in Figure 4.

By analyzing and comparing Figure 9(a-c), it can be seen that Figure 9(a) is the test result of 0.5 mm deep grooving defect on the type A artificial simulation welding test block. With this parameter setting, the actual type A welded joint is detected. By comparing with the red

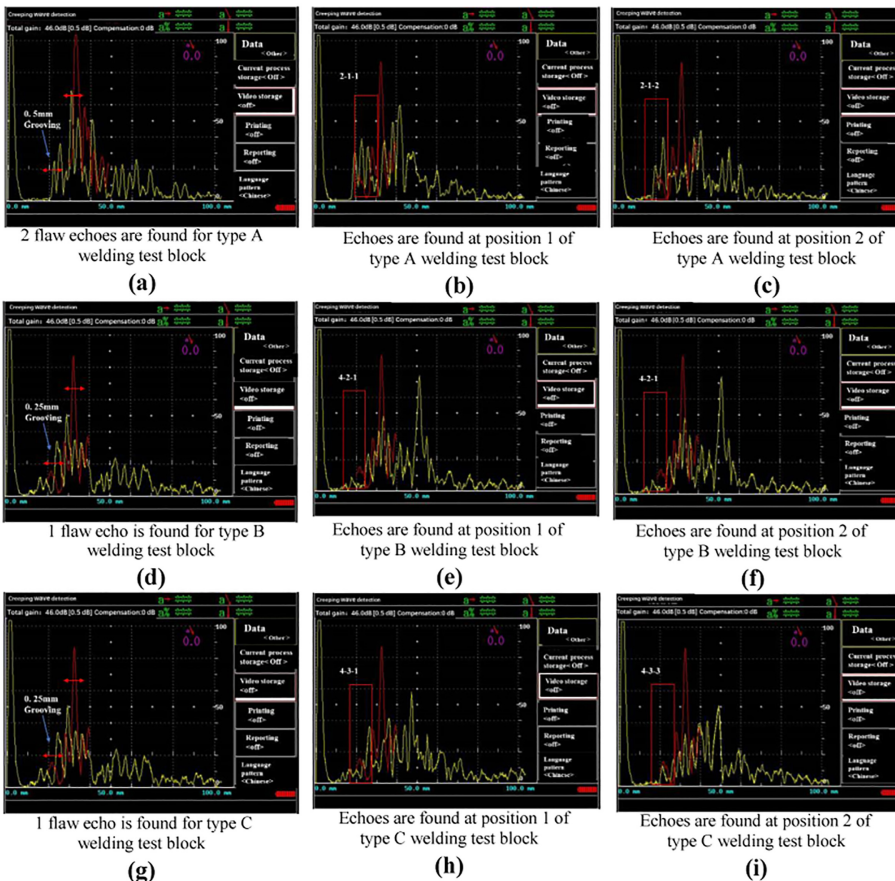


Figure 9.
Creeping wave
detection results of
artificial defect test
block and actual
welded joint

profile welding structure echo, it is found that there is a flaw echo in the gate in the type A welding test block with excess weld metal on the reinforcement of weld, and its defect signal amplitude is the same as the grooving size of 0.5 mm deep surface. As there is no crack on the weld surface, the signal of these defects can be judged as incomplete penetration of the root.

Similar to the detection method of type A welding test block with excess weld metal, [Figure 9\(d\)](#) is the test result of 0.25 mm deep grooving defect on the type B artificial simulation welding test block. According to this, the parameters are set to detect the actual type B welded joint. As can be seen from [Figure 9e and f](#), almost no flaw echo greater than 0.25 mm deep surface grooving is found in the type B welding test block with excess weld metal, so no defect is detected in type B welding test block in this area.

It can be seen from [Figure 9\(g–i\)](#) that in the type C welding test block with excess weld metal, flaw echo is found in some areas, but its signal amplitude is greater than 0.25 mm and slightly smaller than 0.5 mm deep surface grooving flaw echo, and defect echoes are not found in some areas. Therefore, local shallow root incomplete penetration is found for type C welding test block.

3.4 Tensile test

In order to verify the accuracy of the ultrasonic creeping wave detection results, tensile destructive test is carried out for comparison and verification. The creeping wave detection sample mentioned in 2.3.3 shall be made into the tensile test sample of welded joint according to the standard GB/T 2651—2008/ISO 4136: 2001 *Tensile Test Methods on Welded Joints*, and the base metal sample with the same thickness as the sheet in the weld structure shall be selected to fabricate the tensile test sample of base metal. The dimension of samples is shown in [Figure 10](#). The tensile test results are shown in [Table 2](#) and [Figure 11](#).

It can be seen from [Table 2](#): type A sample is broken in the base metal area, type B and C samples are broken in the heat affected zone, without breaking on the weld. It indicates that the weld with pores and incomplete penetration defects shown by X-ray testing is not the weakest area of the welded joint.

According to the design requirements of aluminum alloy welding, the weld strength shall reach 80–95% of the required base metal strength index, while the yield strength and tensile strength index of the base metal shall be greater than or equal to 205 MPa and greater than or equal to 245 MPa, respectively. It can be seen from [Table 2](#) that type B and C base metals meet the strength requirements for the base metal; the tensile strength of the weld of three kinds of test blocks also meets the requirements of 80–95% of the base metal strength (196–233 MPa).

It can also be seen from the tensile curve in [Figure 11](#) that the elongation of each welded joint is obviously reduced relative to the base metal, but the joint strength is not significantly reduced. It indicates that the pores and incomplete penetration defects in the above-mentioned welds are not sufficient to affect the design strength of the welded joints.

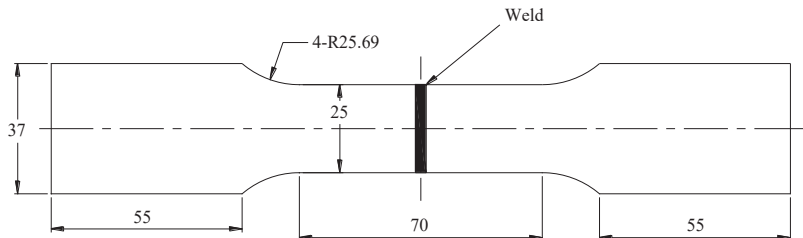


Figure 10.
Machining of tensile
samples (unit: mm)

Sample specification and number	Sample thickness/mm		Sample width/mm	Excess weld metal/mm	Tensile strength/MPa	Fracture location	
	d_1	d_2					
Type A	1#	2.83	3.35	25.02	0.8	294.264	Location of base metal
	2#	2.83	3.37	24.97	0.8	300.286	Location of base metal
Type B	1#	2.36	2.56	25.06	0.57	262.943	Heat affected zone
	2#	2.36	2.56	25.10	0.56	266.856	Heat affected zone
	3#	2.36	2.56	25.05	0.58	271.762	Heat affected zone
	4#	2.36	2.56	25.00	0.78	267.576	Heat affected zone
Type C	1#	2.81	2.36	25.04	0.78	260.689	Heat affected zone
	2#	2.81	2.36	25.06	0.73	256.841	Heat affected zone
	3#	2.81	2.36	25.02	0.82	265.611	Heat affected zone
	4#	2.81	2.36	25.01	0.77	259.629	Heat affected zone
Type B base metal	1#	2.43		25.00		285.292	
	2#	2.43		25.05		281.344	
Type C base metal	1#	2.36		25.02		288.441	
	2#	2.36		25.02		282.200	

Table 2.
Mechanical tensile results

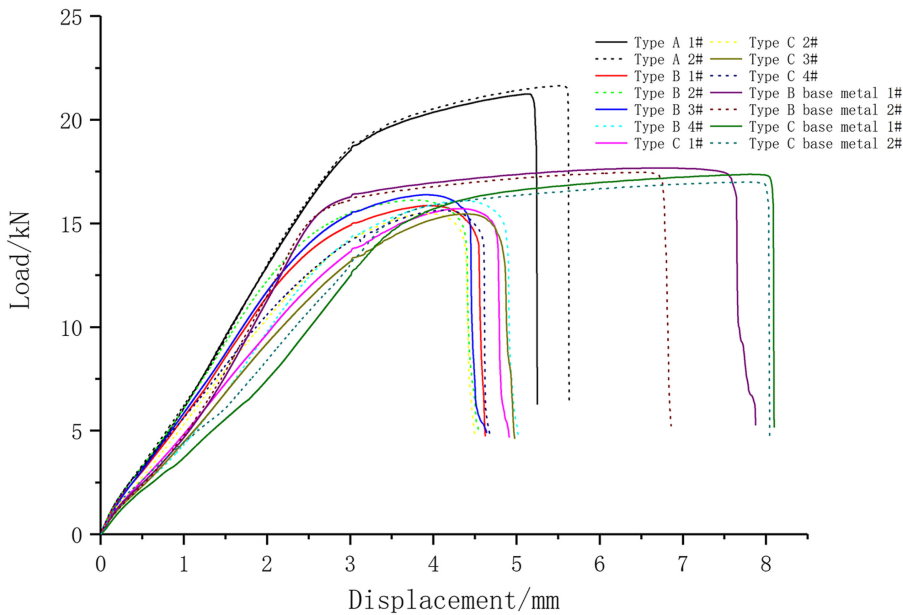


Figure 11.
Mechanical tensile displacement – load curve

3.5 Fracture analysis

The ultrasonic detection results in Figure 9 show that there are various degrees of incomplete penetration defects inside the welds of type A and C samples. In order to verify the accuracy of the ultrasonic detection results in Figure 9, it is necessary to check the fracture at the weld centerline. For samples of types A, B and C after mechanical tensile, the bending test is carried out with the weld centerline as the fulcrum to obtain the weld fracture, as shown in Figure 12.

RS
1,1

110

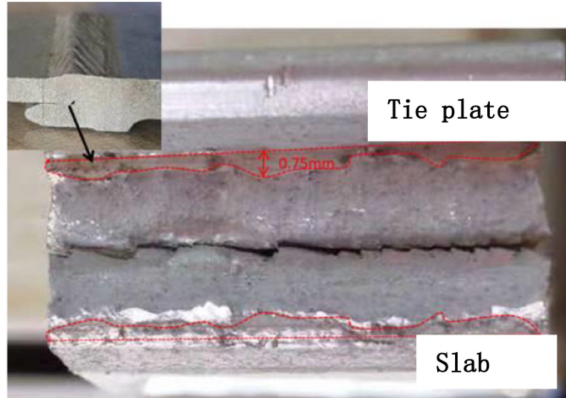


Photo of fracture of longitudinal section of
weld of type A sample
(a)

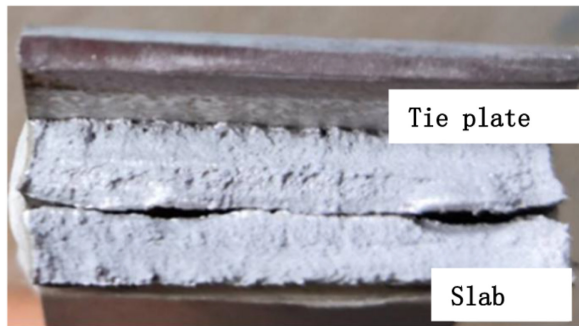


Photo of fracture of longitudinal section of
weld of type B sample
(b)

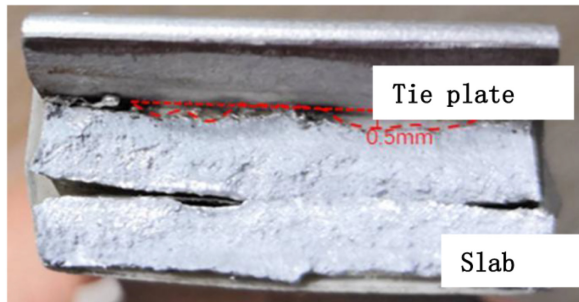


Photo of fracture of longitudinal section of
weld of type C sample
(c)

Figure 12.
Fracture

It can be seen from the fracture of [Figure 12\(a\)](#) that the butt plate of type A sample is thick and there is incomplete penetration at the root; the incomplete penetration area of the root is marked in red-dashed line in the section fracture picture of welds. The maximum depth of incomplete penetration measured is about 0.75 mm, which is corresponding to the 0.5 mm deep equivalent defect detected by ultrasonic detection (see [Figure 9c](#)). There are many porosity defects in the section, and these dispersed pores have no obvious influence on the welding strength.

It can be seen from [Figure 12\(b\)](#) that there is no incomplete penetration defect at the root at the fracture of butt weld section of type B sample, which is corresponding to the equivalent defect with a depth of less than 0.25 mm detected in the ultrasonic detection results (see [Figure 9e](#)). Some porosity defects can be found at the section, and some pores have no obvious influence on the welding strength.

It can be seen from [Figure 12\(c\)](#) that there are local incomplete defects at the root of butt weld of type C sample, as shown in red-dashed line in the figure, which basically corresponds to ultrasonic detection results of grooving equivalent exceeding 0.25 mm deep and less than 0.5 mm deep (see [Figure 9h and i](#)).

3.6 Destructive and NDT results

- (1) Types of defects in weld: The detection results of fracture section show that incomplete penetration defects and a small amount of porosity defects can be found in the weld of aluminum alloy-MIG hybrid welding.
- (2) The results of ultrasonic creeping wave and X-ray testing are highly consistent with the results of fracture section.
- (3) Effect of defects on tensile strength: By testing the welding quality of butt welds with three different thickness combinations, it is found that the thickness of type A sample is large, and the root incomplete penetration defect equivalent to 0.5 mm grooving depth has no effect on strength; type B and C samples fracture in the heat affected zone, the main reason is that the softening of the heat-affected zone reduces the load-carrying capacity of the whole joint, rather than small porosity and shallow incomplete penetration defects. In addition, the unpolished reinforcement of weld will counteract the adverse effects of small porosity and shallow incomplete penetration defects on welding strength to a certain extent.

4. Conclusions

- (1) Fracture observation results show that incomplete penetration is a defect with high probability in hybrid welding. Besides incomplete penetration, a small number of dispersed pores with small size are also found, and no other defects are found. X-ray has a good detection effect on porosity and incomplete penetration defects, but it cannot meet the requirements of on-site detection of aluminum alloy thin-walled profile welding structure of high-speed train body due to its special detection mode and protection and slow detection speed. It can be used as an auxiliary detection means and a small amount of spot checks are carried out when necessary.
- (2) For butt welds of thin-walled profile, due to the limitation of welding structure, it is difficult to carry out effective detection by various existing ultrasonic detection technologies. Therefore, the creeping wave detection method is proposed, and the special creeping wave probes with higher frequency (5 MHz) and small size

(6 mm × 4 mm) wafers are designed through simulation and optimization test. Ultrasonic creeping wave detection technology is developed by using profile welding structure contrasting test block and artificial defect welding test block with reinforcement of weld. The detection results show that this detection technology overcomes the adverse effects of profile welding structure and reinforcement of weld (0.5–0.8 mm) on ultrasonic creeping wave detection and shows the advantages of creeping wave technology in detecting welds with reinforcement of weld. The creeping wave detection can find incomplete penetration defects with an equivalent value greater than or equal to 0.25 mm in thin-walled (2–4 mm) hybrid welding.

- (3) Through comparison of destructive and nondestructive testing results, it is found that the correspondence between flaw echo of creeping wave detection and incomplete penetration defects found in X-ray testing and fracture observation is good, and no missing detection and false alarm are found.
- (4) The tensile test shows that incomplete penetration with an equivalent smaller than or equal to 0.5 mm has no impact on the tensile strength of welds. The fracture occurs in the base metal or heat-affected zone, which meets the design requirement that the joint strength is greater than 85% of the base metal strength.
- (5) In order to ensure the safe service of laser-MIG hybrid welding of aluminum alloy sheet profiles of high-speed trains, nondestructive testing is required for welds; the ultrasonic creeping wave detection is a test method with better effect, and the test emphasis is the detection of incomplete penetration defects. It is recommended to take the echo amplitude of 10 mm × 0.2 mm × 0.5 mm nicks as the criterion for judging whether the weld is qualified.

References

- Cai, G., Shen, J., Sha, G., Zhang, B., Zhu, H., Chen, X., & Liu, C. (2018). The formation mechanism and characteristics of the delayed wave echoes in the slender piece by Axial Ultrasonic inspection. *Nondestructive Testing*, 40(7), 177–8.
- Chen, H., Gou, G., Zhu, Z., Yang, T., & Xiong, J. (2015). Laser-compound MIG welding process and its application status in the field of rail transit. *Electric Welding Machine*, 45(5), 11–14.
- Gan, Z., Fang, X., Yu, G., Yu, Y., & Su, J. (2014). Creeping wave testing for weld of thin-walled high-frequency electric resistance welded pipe. *Welded Pipe and Tube*, 37(2), 33–37.
- Li, G., & Han, X. (2004). The elding echnology for tailess teel ar ody and ts evelopment. *Locomotive and Rolling Stock Technology*, 1, 1–4.
- Sony, B., Balasubramanian, T., & Pardikar, R. J. (2003). Ultrasonic study for detection of inner diameter cracking in pipeline girth welds using creeping waves. *International Journal of Pressure Vessels and Piping*, 2, 139–146.
- Wang, Y., & Chen, H. (2010). Development trend of Al alloy on high speed train. *Electric Welding Machine*, 40(5), 9–16.
- Zhang, Z. (2016). *Study on Microstructures and Properties of Laser Welded 5754-h32 Aluminum Alloy Joints*. Changchun: Jilin University.
- Zeng, Z., Shi, Z., & Shi, Y. (2009). Experimental research on butt-welding deformation of thick plates in large steel structure. *China Railway Science*, 30(3), 33–39.
- Zhang, Y., & Lian, D. (2010). Testing trials for thin-walled welding with creeping wave technique. *Nondestructive Testing*, 32(8), 631–633.

Zhang, Z., Zhan, H., & Ma, L. (2019). Experimental study on Ultrasonic testing of thin-wall aluminum profile laser-MIG composite welded joints. *Manufacturing Technology Machine Tool*, 6, 154–159.

Further reading

State Grid Corporation of China (2012). *Q/GDW 707—2012 Code for Ultrasonic Inspection and Evaluation of Butt Welds of Thin-wall Steel Pipes for Transmission Line Tower*. Beijing: China Electric Power Press.

State Grid Corporation of China (2016). *Q/GDW 1384—2015 the Manufacturing Code for Transmission Line Steel Tubular Tower*. Beijing: China Electric Power Press.

Corresponding author

Fang Liu can be contacted at: liufang@imr.ac.cn